American Journal of Biochemistry and Biotechnology

Original Research Paper

# Separation, Purification and Anti-aging Activity of Tobacco Polysaccharides

[1]Mengyue Huang, [1] Jingwu Song, [1] Shuaishuai Chang, [1] Xuanhao Lei, [1]Jian Ge and [2] Fuzhao Nian

[1]College of Life Sciences, China Jiliang University, Hangzhou, China
[2]College of Tobacco, Yunnan Agricultural University, Kunming, China

*Article history*
Received: 16-07-2024
Revised: 12-10-2024
Accepted: 28-09-2024

Corresponding Author:
Jian Ge
College of Life Sciences, China Jiliang University, Hangzhou, China
Email: gejian@cjlu.edu.cn

**Abstract:** To separate tobacco polysaccharides and investigate their antioxidant and anti-aging properties, crude tobacco polysaccharides were extracted from raw tobacco using hot water, followed by purification through DEAE-52 cellulose column chromatography. The molecular weight and monosaccharide composition of the isolated polysaccharides were analyzed using HPGPC and HPLC. The antioxidant activities of these tobacco polysaccharides were tested using DPPH, ABTS, hydroxyl radicals scavenging test, and total reducing power. HepG-2 cells were treated with D-galactose (D-gal) to establish a senescence model. The anti-aging effects of tobacco polysaccharides were examined through Superoxide Dismutase (SOD) activity assays, Malondialdehyde (MDA) content analysis, qRT-PCR for Sirt1 and Nrf2 mRNA expression. The study found that the molecular weights of tobacco polysaccharides YCH-1, YCH-2, and YCH-3 were 61,708, 66,462, and 69,932 Da, respectively and they exhibited similar monosaccharide type distributions. Tobacco polysaccharides demonstrated strong, dose-dependent antioxidant activities. Cell-based experiments have revealed that these tobacco polysaccharides significantly counteract the senescence of HepG-2 cells induced by D-gal by enhancing SOD levels, while concurrently decreasing MDA content and reducing β-galactosidase positivity rates. This effect may be attributed to elevated mRNA expression levels of Sirt1 and Nrf2 genes within treated cells thereby facilitating their antioxidative functions alongside anti-aging benefits. These findings indicate that the tobacco polysaccharides exhibit significant antioxidant properties and potential anti-aging effects, providing insights into the comprehensive utilization of tobacco resources.

**Keywords:** Tobacco Polysaccharides, Separation, Purification, Antioxidant Activity, Anti-Aging Activity

## Introduction

Tobacco, also known as tobacco leaves, Danbagu, Huanhuncao, is a traditional economic crop with a long history (Zou *et al*., 2021). As the cigarette industry is growing, the scale of tobacco planting has been extended. During tobacco cultivation and processing, large amounts of low-quality tobacco and its by-products are often left unused, discarded, or burned, leading to significant resource wastage. The current research on polysaccharides extraction, development, and utilization of tobacco waste is still little (Jing *et al*., 2016). Consequently, investigating the development and application of polysaccharides from tobacco waste holds considerable significance for enhancing resource efficiency while mitigating environmental impacts.

The aging process is complex (Cai *et al*., 2022). Key contributors to aging include oxidative stress, diminished immune function, chronic inflammation, and dysbiosis of intestinal flora (Du *et al*., 2021). The free radical damage theory suggests that an imbalance between oxidative stress and antioxidant defense promotes cellular aging, while preserving the balance of free radicals and oxidative stress may slow down this process (Campisi *et al*., 2019). As natural antioxidants, plant polysaccharides exhibit promising anti-aging properties (Zhao *et al*., 2023). Previous studies have also demonstrated tobacco polysaccharides possess significant antioxidant and lipid-lowering activities (Chang *et al*., 2024). The potential anti-aging effects of tobacco polysaccharides prompt further inquiry and warrant comprehensive investigation.

In this experiment, crude tobacco polysaccharides were extracted, then purified and separated using trichloroacetic acid, macroporous resin, and DEAE cellulose column chromatography. Their molecular weight and monosaccharide profile were analyzed using

Science Publications

© 2025 Mengyue Huang, Jingwu Song, Shuaishuai Chang, Xuanhao Lei, Jian Ge, and Fuzhao Nian. This open-access article is distributed under a Creative Commons Attribution (CC-BY) 4.0 license.

HPGPC and HPLC. The antioxidant activities of tobacco polysaccharides were assessed in vitro. The anti-aging effects and mechanisms were probed in D-gal induced HepG-2 cell senescence model by β-galactosidase staining, as well as the SOD activity measurement, the MDA content analysis and qRT-PCR for Sirt1 and Nrf2 mRNA expression. These studies offer valuable insights into the utilization of tobacco resources.

## Materials and Methods

### *Materials*

Samples from Yunnan Agricultural University were provided for tobacco analysis. The HepG-2 human liver cancer cell line was sourced from the Cell Resource Center, in Shanghai, China. We obtained dialysis bags, DPPH, and ABTS from the Yuanye Biotechnology Company, Ltd., in Shanghai, China. Monosaccharide standards were obtained from Sigma, USA.

### *Preparation of Tobacco Polysaccharides*

Firstly, we crush the tobacco leaves to obtain tobacco powder. Then, we place the tobacco powder into a water bath at 70°C to extract polysaccharides. After 4 h of extraction, the polysaccharide extract was filtered to remove residues and concentrated to a specific volume. To obtain the polysaccharide precipitate, absolute ethanol was added to the concentrated solution at a volume ratio of 4:1. The crude polysaccharide was obtained by freeze-drying the precipitate and then crude polysaccharide was dissolved to create a 4 mg/mL solution. To remove proteins, 15% trichloroacetic acid solution was added for deproteinization, followed by centrifugation at 4000 rpm to separate and discard the protein precipitates. A 2.5% volume fraction of AB-8 macro-porous resin was introduced into the polysaccharide solution to eliminate pigment impurities by stirring with an electric stirrer for 2 h. Then, the supernatant was concentrated to 100 mL. To obtain deproteinized and decolorized polysaccharides, ethanol at four times the concentrate volume was added and incubated for 12 h to facilitate precipitation.

We have prepared a 20 mg/mL solution of the deproteinized and decolorized polysaccharide and injected it into a DEAE-52 cellulose column at a regulated speed. The solution underwent sequential elution with distilled water, 0.2 mol/L NaCl solution, and 0.4 mol/L NaCl solution. A total of 35 tubes were collected per gradient and the number of tubes was documented. The sugar content in each tube was monitored and identified according to Yan's method (2023). The eluted components were concentrated to a specific volume and dialyzed for 48 h using a 3500 Da molecular retention dialysis bag (Wei *et al*., 2023). The purified tobacco polysaccharide components, YCH-1, YCH-2, and YCH-3, were obtained via vacuum freeze-drying.

### *Determination of Sugar and Uronic Acid Content in Tobacco Polysaccharides*

We determined the sugar content by employing the phenol-sulfuric acid method. Initially, preparations were made of a glucose standard solution at 0.1 mg/mL and a 5% phenol solution. Then, different concentrations of the glucose standard were subjected to absorbance at 490 nm, followed by plotting a standard curve. This is done by determining the total sugar content through the preparation of the tobacco polysaccharide solution at 100 μg/mL, measuring its absorbance and substitution in the equation of the glucose standard curve.

We determined the uronic acid content in tobacco polysaccharides following Zhao *et al*. (2017). Initially, solutions of 1.00 mg/mL galacturonic acid standard, 1.50 mg/mL meta-hydroxyphenyl, and sodium tetraborate/sulfuric acid were prepared. A 0.5 mL sample of the galacturonic acid standard solution was measured and transferred into a 10 mL volumetric flask. The volume was adjusted to the mark with water and mixed thoroughly. Galacturonic acid standard solutions were prepared and transferred into a stoppered test tube. 5.5 mL of sodium tetraborate/sulfuric acid solution was added and heated in the boiling water bath for 5 min. After cooling, 100 μL of meta-hydroxyphenyl solution was added and shaken. Then, we prepared a blank solution and measured its absorbance. Using the content of uronic acid and absorbance as references, a standard curve was plotted. According to the above method, the polysaccharide sample solution was prepared and the absorbance was recorded and compared to the standard curve to determine the uronic acid content.

### *Analysis of Average Molecular Weight of Tobacco Polysaccharides*

Using the HPGPC method, we determined the molecular weight of tobacco polysaccharides. A 10 mg/mL polysaccharide solution was purified by filtering it through a microporous membrane to eliminate impurities. For the chromatographic separation, a chromatographic column with an 8 μm particle size was utilized and the mobile phase consisted of a solution containing 0.2 mol/L $NaNO_3$ and 0.001 mol/L $NaH_2PO_4$.

### *Investigation of Monosaccharide Profiles in Tobacco Polysaccharides*

The monosaccharide profile was analyzed using HPLC, as described by Tian *et al*. (2023). Introduce 10 mg of polysaccharide into a 10 mL hydrolysis tube, followed by the addition of 5 mL of trifluoroacetic acid at a concentration of 2 mol/L. Seal the tube with nitrogen and subject it to hydrolysis at a temperature of 110°C. Following cooling, 1 mL of the hydrolysate was combined with 1 mL of methanol and dried with nitrogen in a 70°C water bath to eliminate trifluoroacetic acid. Subsequently,

1 mL of 0.3 mol/L NaOH was added to dissolve the residue, resulting in the polysaccharide solution for testing. Add 400 μL propylene glycol methyl ether propionate methanol solution to 400 μL mixed monosaccharide standard solution or polysaccharide sample solution. The mixture was heated and then cooled to room temperature. Subsequently, 400 μL of 0.3 mol/L HCL was added for neutralization. Then, 1 mL of distilled water and an equivalent amount of chloroform was added, vigorously mixed, and then allowed to settle for phase separation. The chloroform layer was discarded. The aqueous solution was filtered using a 0.45 μm microporous membrane before HPLC injection analysis.

### *DPPH Free Radical Scavenging Assay*

Sample solutions of YCH-1, YCH-2, and YCH-3 were prepared at concentrations of 0.5, 1, 2, 3, and 4 mg/mL. A 0.5 mL DPPH solution in anhydrous ethanol was combined with the 0.5 mL sample solution. The absorbance at λ = 517 nm was measured after a 30-minute reaction period in the dark. Ascorbic acid ($V_c$) served as a positive control. The DPPH free radical scavenging rate was determined using the formula provided by Gao *et al*. (2022):

$$DPPH\ scavenging\ rate(\%) = \left[\left(1-\left(A_i - A_j\right)/A_0\right)\right]\times 100 \quad (1)$$

where, $A_0$ represents the absorbance of the reaction mixture solution in the absence of the sample, $A_i$ represents the absorbance of both the sample and the DPPH solution. $A_j$ represents the absorbance of the solution without *DPPH*.

### *ABTS Free Radical Scavenging Assay*

A 7.2 mmol/L ABTS stock solution was combined with a 2.4 mmol/L $K_2S_2O_8$ solution for incubation. After allowing the mixture to react for 14 h, it was diluted to a pH of 7.4 to obtain the ABTS working solution. Sample solutions with concentrations of 0.5, 1, 2, 3, and 4 mg/mL were prepared using YCH-1, YCH-2, and YCH-3. The reaction proceeded at room temperature for 20 min and the absorbance ($A_i$) was measured at 734 nm. Instead of sample solution, 0.2 mL anhydrous ethanol was used to calculate the result as $A_0$. The *ABTS* scavenging rate was calculated using the following formula (Kakar *et al*., 2022):

$$ABTS\ scavenging\ rate(\%) = \left[\left(1-A_i/A_0\right)\right]\times 100 \quad (2)$$

where, $A_0$ represents the absorbance of the reaction mixture solution without a sample, $A_i$ represents the absorbance measured in the sample group.

### *Hydroxyl Radical Scavenging Assay*

Sample solutions were prepared with YCH-1, YCH-2, and YCH-3 concentrations between 0.5 and 4 mg/mL. A 0.2 mL portion of a mixture containing 6 mmol/L $FeSO_4$ and an equal concentration of $H_2O_2$ was blended with 0.2 mL of a polysaccharide solution. Subsequently, a 6 mmol/L salicylic acid-ethanol solution was introduced and then incubated in a water bath at 37°C for a duration of 15 min, followed by measuring the absorbance Ai at 510 nm. The hydroxyl radical scavenging rate was calculated according to Luo *et al.* (2019). The calculation formula is as follows:

$$Scavenging\ Rate(\%) = \left[1-\left(A_i - A_j\right)/A_0\right]\times 100 \quad (3)$$

where, $A_0$ represents the absorbance of the solution without the sample, $_{ai}$ is measured in the sample group. $A_j$ represents the absorbance of the solution without $H_2O_2$.

### *The Reducing Power Assay*

The polysaccharide sample solution of a specific concentration was prepared according to the aforementioned method. 2.5 mL of 0.2 mol/L PBS and 1% potassium ferricyanide solution were combined with a 1-mL sample and then incubated at 50°C for 20 min before being rapidly cooled in cold water. The reaction was halted by adding 2.5 mL of 2.5% trichloroacetic acid, followed by centrifugation at 4000 r/min for 20 min. 2.5 mL of the supernatant was transferred to a new test tube, followed by the addition of 0.5 mL of 0.1% ferric chloride solution and 2.5 mL of deionized water. Absorbances were measured at 700 nm after adding and standing for 10 min. A blank control group was set up where distilled water was used in place of various reagents for the reaction. The reduction degree was determined using the formula provided by Petraglia *et al*. (2023):

$$A700 = A_i - A_0 \quad (4)$$

where, *A*700 is the total reducing power. $A_i$ and $A_0$ represent the absorbance values of the sample group and the blank group, respectively.

### *Screening of D-gal Modeling Concentration*

HepG-2 cells were maintained in DMEM supplemented with 10% FBS and 1% penicillin-streptomycin at 37°C for 24 h in a humidified incubator. Following a conventional culture, the D-gal treatment group received 100 μL of complete medium with D-gal concentrations of 37.5, 75, 150, and 300 mmol/L, while the control group was administered an equivalent volume of normal medium. Cell viability was calculated according to the CCK8 method after 48 h of incubation, identifying the concentration that ensured complete cell survival as the safe level for aging modeling. The formula for calculating the cell survival rate is as follows:

$$Cell\ survival\ rate = A_i / A_0 \times 100 \quad (5)$$

where, $A_i$ is the result measured in the D-gal treatment group. $A_0$ is the result recorded in the control group.

### *Screening of Tobacco Polysaccharides Treatment Concentration*

After 24 h of routine culture, HepG-2 cells were divided into a control group and a treatment group. The control group received 200 μL of complete medium, whereas the treatment group was administered 100 μL of complete medium with D-gal (150 mmol/L) and 100 μL of medium containing YCH-1, YCH-2, and YCH-3 at concentrations of 62.5, 125, 250, 500 and 1000 μg/mL. After a further 48 h incubation, cell vitality was calculated as follows:

$$Cell\ survival\ rate = A_i / A_0 \times 100 \quad (6)$$

Where $A_i$ is the absorbance value measured after treatment with different concentrations of tobacco polysaccharide. $A_0$ represents the absorbance value recorded following cultivation in a standard medium.

### *Effects of Tobacco Polysaccharides on the Production of β-galactosidase in HepG-2 Cells*

After 24 h of routine culture, HepG-2 cells were divided into a control group, a D-gal group, and a polysaccharides group. In the control group, 2 mL of normal medium solution was added. The D-gal group received 2 mL of standard culture medium containing 75 mmol/L D-gal. The YCH-1, YCH-2, and YCH-3 groups were each administered 1 mL of medium containing 150 mmol/L D-gal and 1 mL of medium containing 250 μg/mL of the respective polysaccharide specific to each group. After the cells were cultured for 48 h, they were stained using a β-galactosidase in situ staining kit.

### *Impact of Tobacco Polysaccharides on SOD Enzyme Activity and MDA Levels in HepG-2 Cells*

HepG-2 cells were divided into a control group, D-gal group, and polysaccharides groups as described above. Following treatment, cell lysis was performed and SOD activity along with MDA content was measured as per the kit instructions. Each group had 3 holes set up and the experiment was conducted 3 times.

### *The mRNA Levels of Sirt1 and Nrf2 were Detected by Real-Time Fluorescence Quantitative PCR*

The experimental procedures categorized the cells into three groups: Control, D-gal, and YCH-3. Cell RNA was obtained by the Trizol method 24 h post-drug intervention. The content, purity, and quality of RNA are determined by the ultraviolet spectrophotometer and electrophoresis. The total RNA was reverse-transcribed into cDNA as per kit instructions. Primer sequences specific to Sirt1 and Nrf2 were designed using Premier 6.0 and Beacon Designer 7.8 software and synthesized by Shanghai Sangon Bioengineering Co., Ltd. The primer sequence is shown in Table (1).

**Table 1:** Primer sequences and conditions for real-time PCR

| Gene | Genbank Accession | Primer Sequences (5'to3') | Size (bp) | Annealing (°C) |
|---|---|---|---|---|
| Human GAPDH | NM-002046.5 | CCATGACAACTTT GGTATCGTGGAA<br>GGCCATCACGCCA CAGTTTC | 107 | 60 |
| Human NRF2 | NM-001145412.2 | CAGCCCAGCACAT CCAGTCAG<br>CTGAAACGTAGCC GAAGAAACCTCA | 161 | 60 |
| Human SIRT1 | NM-001142498.1 | GGAGGAGCTGGAT TTGGGACTGAT<br>GGTGGAACAATTC CTGTACCTGCACA | 143 | 60 |

### *Data Analysis*

Experiments were performed in triplicate and results are presented as mean ± standard deviation. The data processing and statistical analysis were conducted using GraphPad Prism version 9.5.1, with a P-value of less than 0.01 considered statistically significant.

## Results

### *Purification and Separation Results of Tobacco Polysaccharides*

The DEAE-52 cellulose column is an anion exchange chromatography column, which can divide the sample into different components according to the charge intensity of the sample. Figure (1) shows the elution curve of tobacco polysaccharides. Three polysaccharide components, YCH-1, YCH-2, and YCH-3, were obtained following elution with distilled water and 0.2 and 0.4 mol/L NaCl solutions. According to the principle of DEAE-52 cellulose column separation, it can be inferred that YCH-1 is a neutral component eluted by distilled water and YCH-2 and YCH-3 are acidic components eluted by NaCl solution.

### *Chemical Composition of Different Components of Tobacco Polysaccharides*

The glucose standard curve, derived using phenol-sulfuric acid methods, is represented by Y = 88.46× +0.405 with an $R^2$ of 0.9939. For galacturonic acid, the standard curve is Y = 0.0393× +0.036 with an $R^2$ of 0.9966. The basic chemical composition of the three samples was analyzed as presented in Table (2). YCH-1, YCH-2 and YCH-3 are purified polysaccharides, as indicated by the significant differences ($p<0.01$) in their results compared to the crude polysaccharide. The uronic acid content was found to be 16.00±0.82% in YCH-1, 18.14±0.49% in YCH-2, and 25.61±1.41% in YCH-3.

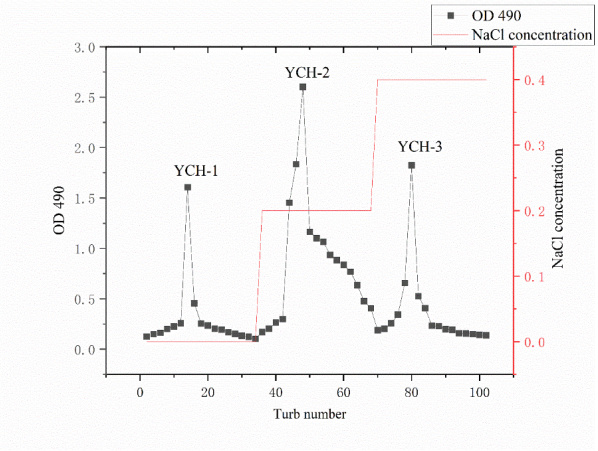


**Fig. 1:** The separation and elution curve of tobacco polysaccharides, three components: YCH-1, YCH-2, and YCH-3

**Table 2:** Chemical composition analysis of tobacco polysaccharides

| Sample | Total sugar content（%） | Uronic acid content（%） |
|---|---|---|
| Crude polysaccharide | 26.82±0.37** | - |
| YCH-1 | 85.93±0.42** | 16.00±0.82** |
| YCH-2 | 81.57±1.15** | 18.14±0.49** |
| YCH-3 | 74.14±0.84** | 25.61±1.41** |

**, the difference is significant at 0.01 level between different samples ($p<0.01$)

### *Average Molecular Weight of Different Components of Tobacco Polysaccharides*

Among various structural indexes of polysaccharides, molecular weight influences the physiochemical properties and activity of polysaccharides. Figure (2) is a result of molecular weight determination of polysaccharide components. The peak molecular mass for YCH-1, YCH-2, and YCH-3 is 61,708 Da (Fig. 2a), 66462 Da (Fig. 2b), and 69932 Da (Fig. 2c), respectively. The molecular weights of these three polysaccharides differ from those of tobacco polysaccharides previously reported in the literature ($6.6517\times10^4$ Da, $2.759\times10^4$ Da) (Chang *et al.*, 2024). The experiment suggests that these three polysaccharides could be novel tobacco polysaccharides.

### *Monosaccharide Composition of Different Components of Tobacco Polysaccharides*

The type, order, and number of monosaccharide residues on the polysaccharide chain constitute the primary structure, which is highly relevant to polysaccharide biological activity. Table (3) presents the comparative molar ratios and HPLC analysis of the monosaccharide compositions for YCH-1, YCH-2, and YCH-3. From the above table, it's clear that YCH-1 contains 10 types of monosaccharides, whereas YCH-2 and YCH-3 contain 12 types of monosaccharides. The kinds of monosaccharides of YCH-2 and YCH-3 are the same, but the relative molar ratio of each monosaccharide is different. Glucose content is high for YCH-1 and YCH-2, but the D-glucuronic acid and galacturonic acid of YCH-3 are relatively high. Compared with YCH-1 and YCH-2, YCH-3 had a higher uronic acid content in its polysaccharides, which was consistent with the determination result of the uronic acid content in the chemical composition of tobacco polysaccharides. This difference of monosaccharides composition and contents may lead to their different spatial structure and different biological activity of tobacco polysaccharides, but the definite structure-activity relationship needs further study as well.

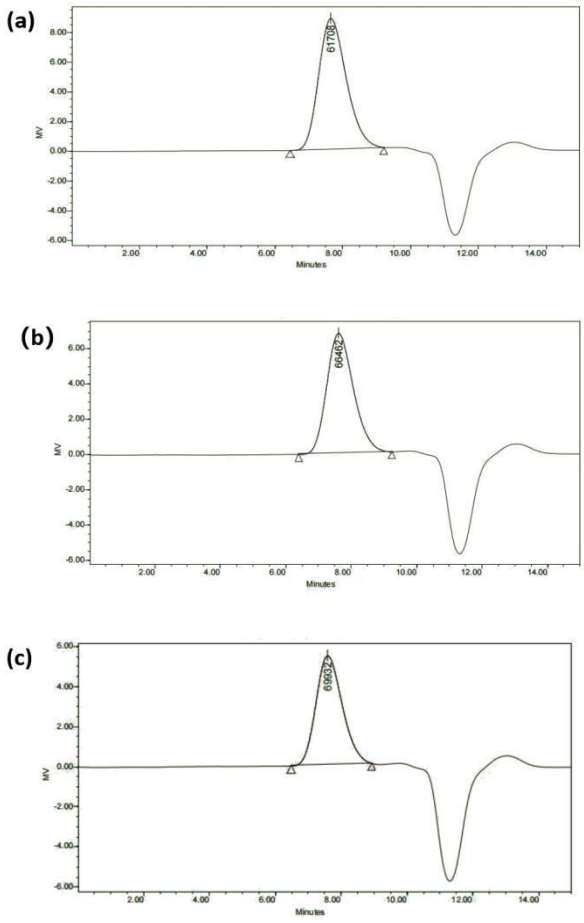


**Fig. 2:** Molecular weights of tobacco polysaccharide components. (a) The molecular weight of YCH-1; (b) The molecular weight of YCH-2; (c) The molecular weight of YCH-3

**Table 3:** The relative molar ratio of monosaccharides in tobacco polysaccharides (%)

| Monosaccharide type | YCH-1 | YCH-2 | YCH-3 |
|---|---|---|---|
| L-guluronic acid | 0.029 | 0.024 | 0.032 |
| D-mannuronic acid | 0.007 | 0.024 | 0.028 |
| D-mannose | 0.126 | 0.345 | 0.369 |
| D-glucosamine | 0.039 | 0.099 | 0.093 |
| L-rhamnose | 0.342 | 4.728 | 13.070 |
| D-glucuronic acid | 0.219 | 3.212 | 7.153 |
| D-galacturonic acid | 0.027 | 0.220 | 3.975 |
| D-glucose | 95.956 | 61.801 | 39.892 |
| D-galactose | 1.784 | 18.830 | 25.045 |
| D-xylose | 0.000 | 0.225 | 0.349 |
| L-arabinose | 1.470 | 10.433 | 9.788 |
| L-fucose | 0.000 | 0.058 | 0.206 |

## *Antioxidant Activity of Tobacco Polysaccharides*

The DPPH radical scavenging rates of YCH-1, YCH-2, and YCH-3, as shown in Fig. (3a), increased with the increase in sample concentration, demonstrating a dose effect. When the concentration of samples was 4 mg/mL, YCH-1, YCH-2, and YCH-3 DPPH radical scavenging rates respectively reached 58.48, 63.14 and 78.65%.

Figure (3b) displays the ABTS radical scavenging rates of YCH-1, YCH-2 and YCH-3. Each of the three polysaccharides exhibited a dose-dependent increase in ABTS radical scavenging rate as the sample concentration increased. In particular, the ABTS radical scavenging rate of YCH-3 was markedly greater than those of YCH-1 and YCH-2 at the concentration of 4 mg/mL.

Hydroxyl radicals, found in most cells, are essential for evaluating antioxidant activity. Hydroxyl radical scavenging ability data are displayed in Fig. (3c). The results indicated that YCH-1, YCH-2, and YCH-3 exhibited a significant dose-dependent increase as sample concentrations rose from 0.5-4 mg/mL. Moreover, the three components of tobacco polysaccharides effectively scavenged hydroxyl radicals.

The reducing power is also employed to gauge the antioxidant efficacy of polysaccharides. As depicted in Fig. (3d), YCH-1, YCH-2, and YCH-3 demonstrated an increase in reducing power proportional to concentration (0.5-4 mg/mL), indicating a positive correlation between concentration and effect. Nevertheless, compared with Vc, their reducing power was appreciably lower.

YCH-1, YCH-2, and YCH-3 exhibit antioxidant activity, albeit lower than the antioxidant activity of Vc under identical conditions. Moreover, YCH-3 has better antioxidant capacity than YCH-1 and YCH-2, possibly due to variations in the chemical composition and structure of its polysaccharides. The study's findings suggest that YCH-1, YCH-2, and YCH-3 could be developed as antioxidants. This study provides important insights for future research on the structure-activity relationship of tobacco polysaccharides.

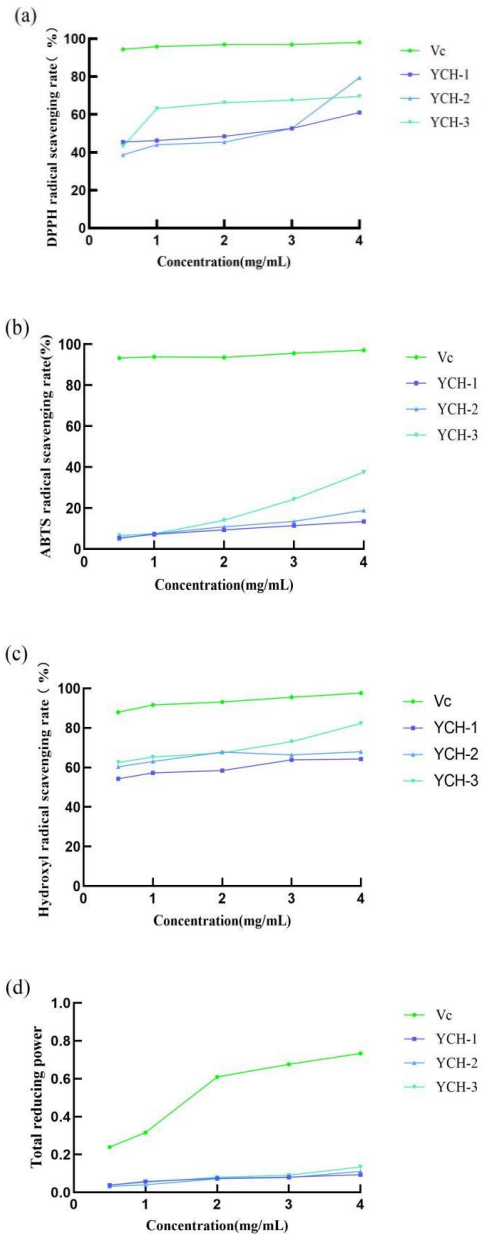


**Fig. 3:** The antioxidant activity outcomes for YCH-1, YCH-2 and YCH-3. (a) (b) and (c) are DPPH, ABTS, and Hydroxyl radicals scavenging rate, respectively; (d) is total reducing power (VC was utilized as the positive control in this study)

## *Establishment of HepG-2 Cell Senescence Model*

The CCK-8 test results are illustrated in Fig. (4). As D-gal concentration increased, the cell survival rate decreased. Cell survival was over 98% at 75 mmol/L D-gal, but decreased to 73.62% at 150 mmol/L, showing a significant difference between the two groups ($p<0.01$). Therefore, 75 mmol/L was identified as the most appropriate concentration for D-gal-induced modeling.

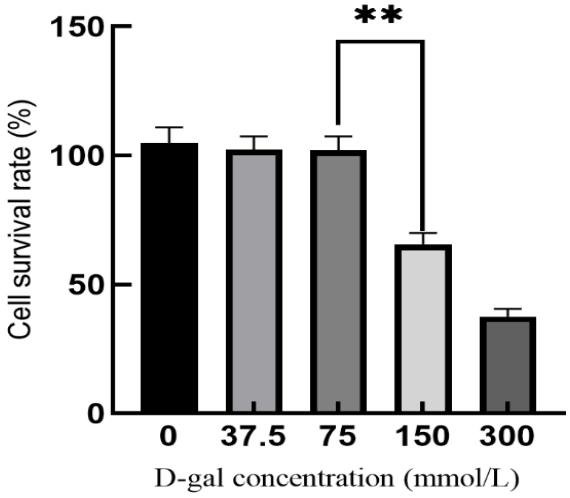


**Fig. 4:** The survival rate of HepG-2 cells induced by different concentrations of D-gal. **p<0.01 for comparison between the two groups

### *Determination of treatment Concentration of Tobacco Polysaccharides*

Figure (5) presents the CCK 8 test results. Cell survival rates for YCH-1, YCH-2, and YCH-3 were >95% at 250 μg/mL. At a concentration of 500 μg/mL, however, the survival rate decreased to around 80%, with a statistical difference ($p<0.01$). Given that excessively high drug concentrations can cause cell death, the treatment concentration for tobacco polysaccharides was determined to be 250 μg/mL.

### *Tobacco Polysaccharides Significantly Reduced the Production of β-galactosidase in HepG-2 Senescent Cells*

β-galactosidase, a common senescence marker, was observed under an optical microscope in HepG-2 senescent cells treated with YCH-1, YCH-2, and YCH-3. The findings are presented in Fig. (6). Figures (6a-e) are the control group, D-gal model group, YCH-1 treatment group, YCH-2 treatment group, and YCH-3 treatment group, respectively. From the figure, it is evident that the β-galactosidase activity in the D-gal model group has increased significantly compared to the control group, with numerous cells stained blue. Based on the staining results of the two groups, we have successfully established a senescent cell model. Compared to the model group, the YCH-1, YCH-2, and YCH-3 groups significantly reduced β-galactosidase activity and decreased the count of β-galactosidase positive cells in HepG-2 senescent cells, indicating that tobacco polysaccharides have anti-aging activity.

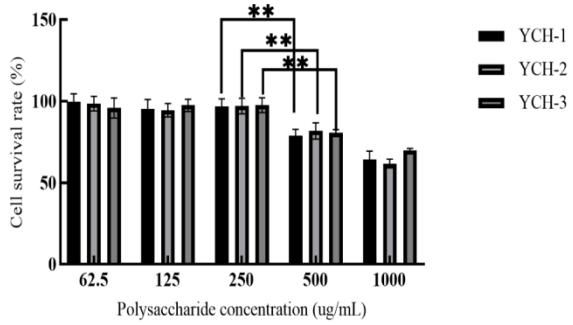


**Fig. 5:** The survival rates of cells following treatment with YCH-1, YCH-2 and YCH-3. **p<0.01 for comparison between the two groups

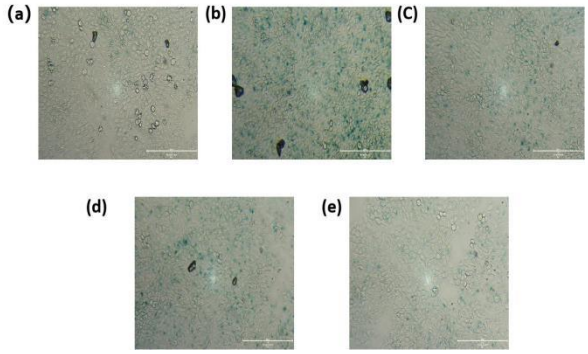


**Fig. 6:** The effects of YCH-1, YCH-2, and YCH-3 on β-galactosidase staining in HepG-2 cells. (a): Control group; (b): Model group; (c): YCH-1 treatment group (250 μg/mL); (d): YCH-2 treatment group (250 μg/mL); (e): YCH-3 treatment group (250 μg/mL)

### *Tobacco Polysaccharides Increased SOD Activity and Lessened MDA Content in HepG-2 Senescent Cells*

SOD is a crucial enzyme in the antioxidant system, significantly contributing to the delay of aging (Li *et al*., 2019). MDA, an intermediate product of free radical-induced damage to unsaturated fatty acids, indicates the extent of oxidative damage (Lin *et al*., 2019). The measurement results of SOD and MDA activity for each group are shown in Table (4). Compared to the control group, the model group exhibited a reduction in SOD activity and an increase in MDA content. In the YCH-1, YCH-2, and YCH-3 groups, we can clearly observe that after treatment with polysaccharides, the SOD activity and MDA content were reversed, approaching those observed in the control group. The findings suggest that tobacco polysaccharides enhance the antioxidant capacity of senescent HepG-2 cells.

**Table 4:** Effects of tobacco polysaccharides on SOD activity and MDA content in HepG-2 cells

| Group | SOD / (U/mg protein) | MDA / (nmol/mg protein) |
|---|---|---|
| Control group | 44.813±1.213 ** | 3.985±0.429 ** |
| Model group | 29.480±0.983 | 5.077±0.830 |
| YCH-1 group | 35.068±0.762 ** | 4.754±1.283** |
| YCH-2 group | 38.810±1.283 ** | 4.472±1.817** |
| YCH-3 group | 41.961±1.238 ** | 4.595±0.773** |

**, the difference is significant at 0.01 level compared with the model group ($p<0.01$)

**Table 5:** Relative expression levels of Sirt1 and Nrf2 in HepG-2 cells

| Group | Sirt1 | Nrf2 |
|---|---|---|
| Control group | 0.998±0.059** | 0.958±0.077 ** |
| Model group | 0.721±0.091 | 0.796±0.085 |
| YCH-3 group | 0.818±0.067 ** | 0.802±0.076 ** |

**, the difference is significant at 0.01 level compared with the model group ($p<0.01$)

### *Tobacco Polysaccharides Markedly Elevated Sirt1 and Nrf2 mRNA Levels in Senescent HepG-2 Cells*

Silent information regulator 1 (Sirt1) regulates the aging process of organisms by modulating oxidative stress, inflammatory response, apoptosis, autophagy, and other signaling pathways, which are associated with longevity (Cui *et al*., 2022). Nrf2, or nuclear factor erythroid 2-related factor 2, serves as a key transcription factor in regulating cellular redox balance. Under stimulation with oxidative stress, it is translocatable into the nucleus where it can bind to the antioxidant response element leading to a transcription of downstream antioxidant genes such as SOD, thus exerting antioxidant effects (Yuan *et al*., 2021). In this study, the Sirt1 and Nrf2 mRNA expression levels were examined using qRT-PCR and presented in Table (5). From the table, we can observe that the expression levels of Sirt1 and Nrf2 mRNA in the model group are lower than those in the control group. However, compared to the model group, the expression levels of Sirt1 and Nrf2 mRNA in the YCH-3 group were significantly higher. ($p<0.01$). The findings suggest that D-gal may induce cellular senescence by downregulating the level of Sirt1 and Nrf2 mRNA. However, tobacco polysaccharides may counteract aging by upregulating these mRNA levels, thereby enhancing SOD and other antioxidant enzyme activities to maintain intracellular redox balance in HepG-2 cells.

## Discussion

This study obtained three new tobacco polysaccharide components, YCH-1, YCH-2, and YCH-3, through extraction, purification, and isolation procedures. These components have similar molecular weights.YCH-1 comprises ten distinct monosaccharides, while both YCH-2 and YCH-3 contain twelve. All three polysaccharides include reducing monosaccharides such as glucose and galactose, with YCH-3 notably enriched in monosaccharides containing uronic acid groups. Results of tests measuring the anti-free radical capacities and reducing the power of these polysaccharides showed that YCH-3 has a marked anti-oxidation effect, a known effect mainly related to differences in its structure and chemical composition. Research indicates that the anti-oxidation properties of polysaccharides are closely related to their physicochemical properties, such as monosaccharide composition and glycosidic bond configuration (Casas-Arrojo *et al*., 2021). Furthermore, research has demonstrated that polysaccharides exhibiting acidic characteristics and having an elevated content of uronic acid tend to possess superior antioxidant properties (Li *et al*., 2021). The study draws together the findings related to the chemical composition, molecular weight, and monosaccharide makeup of polysaccharides to speculate that acidic polysaccharides with a high uronic acid content might have better antioxidant activity. Based on the measurement results of the physicochemical properties of polysaccharides, this study speculates that acidic polysaccharides with a high content of uronic acid may possess better activity. However, establishing a structure-activity relationship will take more work.

Oxidative stress serves as a pivotal factor contributing to cellular senescence. Under typical physiological conditions, a dynamic balance is maintained between oxidation and antioxidation processes. However, aging or exposure to various detrimental stimuli can lead to an overproduction of highly reactive molecules within the body. This imbalance results in oxidative damage surpassing detoxification capabilities which accelerates cellular aging (Hajam *et al*., 2022). D-gal is a stable six-carbon aldose that accumulates intracellularly leading to disrupted glucose metabolism characterized by cell swelling and necrosis and it undermines the body's antioxidant defense mechanisms thereby inducing oxidative stress-related aging phenomena (Li *et al*., 2018). In this experiment, D-gal was employed to induce oxidative stress injury facilitating age-related changes. Results from senescence-associated β-galactosidase staining alongside assessments of SOD activity and MDA levels confirmed the successful establishment of HepG-2 cell senescence models. The enhancement of SOD levels, concurrent with the decrease in MDA content and reduced β-galactosidase positivity rates in HepG-2 cells exposed to D-gal, indicated that tobacco polysaccharides effectively counteract the effects of D-gal. These findings indicate that D-gal-induced senescence in HepG-2 cells is associated with oxidative stress damage. Tobacco polysaccharides alleviate cell senescence by improving the redox state, thereby enhancing the overall antioxidant capacity. The research results of Takaya demonstrated

that Cistanche deserticola polysaccharide treatment reduces the number of β-galactosidase-positive cells, inhibits the production of Reactive Oxygen Species (ROS), and alleviates oxidative stress during the senescence of human dermal fibroblasts (Takaya *et al*., 2023). These findings are similar to those of our study, both confirming the antioxidant and anti-aging activities of polysaccharides.

Sirt1 and Nrf2 are key genes in the field of anti-aging research. This study discovered a statistically significant increase in cellular Sirt1 and Nrf2 mRNA levels under the influence of tobacco polysaccharides compared to the model group. We hypothesize tobacco polysaccharides may act on the key active site of Sirt1, which in turn facilitates the nuclear translocation of Nrf2, thereby enhancing the expression of downstream antioxidant genes, maintaining redox balance, and exerting antioxidant and anti-aging activities. Lee found that Alpinia officinarum enhanced Sirt1 protein expression, leading to the deacetylation of PGC-1α, which subsequently upregulated Nrf2 and antioxidant-related genes. Alpinia officinarum reversed $H_2O_2$-induced senescence of dermal fibroblasts by Sirt1/PGC-1α/Nrf2 signal transduction (Lee *et al*., 2022). Furthermore, Takaya's investigations revealed that Cistanche deserticola polysaccharide mitigated aged characteristics among dermal fibroblasts utilizing Nrf2/HO-1 pathway interactions (Takaya *et al*., 2023). While our current analysis primarily centered on the quantification of mRNA expression levels of Sirt1 and Nrf2, the regulatory mechanism between Sirt1 and Nrf2 remains to be studied.

## Conclusion

This study successfully extracted, purified, and separated three novel tobacco polysaccharide components: YCH-1, YCH-2 and YCH-3. They have similar physicochemical structures. All three compounds showed different antioxidative activity, potentially attributable to variations in chemical composition and structure. Analysis of senescence-associated β-galactosidase staining, SOD activity, and MDA content in HepG-2 cells suggests that tobacco polysaccharides exhibit anti-aging effects. Analysis of Sirt1 and Nrf2 mRNA expression in HepG-2 cells indicates that these polysaccharides may influence anti-aging effects through the Sirt1/Nrf2 signaling pathway. Our research lays a foundation for developing new plant-derived functional foods utilizing tobacco polysaccharides while promoting the efficient use of tobacco resources to mitigate environmental pollution associated with tobacco cultivation.

## Acknowledgment

We thank the Tobacco College of Yunnan Agricultural University for its support and help.

## Funding Information

This research was funded by the National Natural Science Foundation of China (31100499).

## Author's Contribution

**Mengyue Huang:** Project administration, conceptualization, written-original drafted.

**Jingwu Song:** Methodology, software, resources.

**Shuaishuai Chang:** Methodology, software.

**Xuanhao Lei:** Methodology, Investigation, resources.

**Jian Ge:** Funded acquisition, supervision, project administration, written-reviewed and edited.

**Fuzhao Nian:** Supervision, project administration.

## Ethics

The authors declare that they have no conflict of interest.

## References

Cai, Y., Song, W., Li, J., Jing, Y., Liang, C., Zhang, L., Zhang, X., Zhang, W., Liu, B., An, Y., Li, J., Tang, B., Pei, S., Wu, X., Liu, Y., Zhuang, C.-L., Ying, Y., Dou, X., Chen, Y., … Liu, G.-H. (2022). The landscape of aging. *Science China Life Sciences*, *65*(12), 2354–2454. https://doi.org/10.1007/s11427-022-2161-3

Casas-Arrojo, V., Decara, J., de los Ángeles Arrojo-Agudo, M., Pérez-Manríquez, C., & Abdala-Díaz, R. (2021). Immunomodulatory, Antioxidant Activity and Cytotoxic Effect of Sulfated Polysaccharides from Porphyridium cruentum. (S.F.Gray) Nägeli. *Biomolecules*, *11*(4), 488. https://doi.org/10.3390/biom11040488

Campisi, J., Kapahi, P., Lithgow, G. J., Melov, S., Newman, J. C., & Verdin, E. (2019). From discoveries in ageing research to therapeutics for healthy ageing. *Nature*, *571*(7764), 183–192. https://doi.org/10.1038/s41586-019-1365-2

Chang, S., Lei, X., Xie, Q., Zhang, M., Zhang, Y., Xi, J., Duan, J., Ge, J., & Nian, F. (2024). In vitro study on antioxidant and lipid-lowering activities of tobacco polysaccharides. *Bioresources and Bioprocessing*, *11*(1), 15. https://doi.org/10.1186/s40643-024-00729-9

Cui, Z., Zhao, X., Amevor, F. K., Du, X., Wang, Y., Li, D., Shu, G., Tian, Y., & Zhao, X. (2022). Therapeutic application of quercetin in aging-related diseases: SIRT1 as a potential mechanism. *Frontiers in Immunology*, *13*, 943321. https://doi.org/10.3389/fimmu.2022.943321

Du, Y., Gao, Y., Zeng, B., Fan, X., Yang, D., & Yang, M. (2021). Effects of anti-aging interventions on intestinal microbiota. *Gut Microbes*, *13*(1), 1994835. https://doi.org/10.1080/19490976.2021.1994835

Gao, Z., Wu, C., Wu, J., Zhu, L., Gao, M., Wang, Z., Li, Z., & Zhan, X. (2022). Antioxidant and anti-inflammatory properties of an aminoglycan-rich exopolysaccharide from the submerged fermentation of Bacillus thuringiensis. *International Journal of Biological Macromolecules*, *220*, 1010–1020. https://doi.org/10.1016/j.ijbiomac.2022.08.116

Hajam, Y. A., Rani, R., Ganie, S. Y., Sheikh, T. A., Javaid, D., Qadri, S. S., Pramodh, S., Alsulimani, A., Alkhanani, M. F., Harakeh, S., Hussain, A., Haque, S., & Reshi, M. S. (2022). Oxidative Stress in Human Pathology and Aging: Molecular Mechanisms and Perspectives. *Cells*, *11*(3), 552. https://doi.org/10.3390/cells11030552

Jing, Y., Gao, Y., Wang, W., Cheng, Y., Lu, P., Ma, C., & Zhang, Y. (2016). Optimization of the extraction of polysaccharides from tobacco waste and their biological activities. *International Journal of Biological Macromolecules*, *91*, 188–197. https://doi.org/10.1016/j.ijbiomac.2016.05.069

Kakar, M. U., Li, J., Mehboob, M. Z., Sami, R., Benajiba, N., Ahmed, A., Nazir, A., Deng, Y., Li, B., & Dai, R. (2022). Purification, characterization and determination of biological activities of water-soluble polysaccharides from Mahonia bealei. In *Scientific Reports* (Vol. 12, Issue 1, p. 8160). https://doi.org/10.1038/s41598-022-11661-3

Lee, J.-J., Ng, S.-C., Hsu, J.-Y., Liu, H., Chen, C.-J., Huang, C.-Y., & Kuo, W.-W. (2022). Galangin Reverses $H_2O_2$-Induced Dermal Fibroblast Senescence via SIRT1-PGC-1α/Nrf2 Signaling. *International Journal of Molecular Sciences*, *23*(3), 1387. https://doi.org/10.3390/ijms23031387

Li, C., Tan, F., Yang, J., Yang, Y., Gou, Y., Li, S., & Zhao, X. (2019). Antioxidant Effects of Apocynum venetum Tea Extracts on D-Galactose-Induced Aging Model in Mice. *Antioxidants*, *8*(9), 381. https://doi.org/10.3390/antiox8090381

Li, C.-Y., Liu, L., Zhao, Y.-W., Chen, J.-Y., Sun, X.-Y., & Ouyang, J.-M. (2021). Inhibition of Calcium Oxalate Formation and Antioxidant Activity of Carboxymethylated Poria cocos Polysaccharides. *Oxidative Medicine and Cellular Longevity*, *2021*(1), 6653593. https://doi.org/10.1155/2021/6653593

Li, S., Liu, H., Wang, W., Wang, X., Zhang, C., Zhang, J., Jing, H., Ren, Z., Gao, Z., Song, X., & Jia, L. (2018). Antioxidant and anti-aging effects of acidic-extractable polysaccharides by Agaricus bisporus. *International Journal of Biological Macromolecules*, *106*, 1297–1306. https://doi.org/10.1016/j.ijbiomac.2017.08.135

Lin, X., Bai, D., Wei, Z., Zhang, Y., Huang, Y., Deng, H., & Huang, X. (2019). Curcumin attenuates oxidative stress in RAW264.7 cells by increasing the activity of antioxidant enzymes and activating the Nrf2-Keap1 pathway. *PloS One*, *14*(5), e0216711. https://doi.org/10.1371/journal.pone.0216711

Luo, Y., Peng, B., Wei, W., Tian, X., & Wu, Z. (2019). Antioxidant and Anti-Diabetic Activities of Polysaccharides from Guava Leaves. *Molecules*, *24*(7), 1343. https://doi.org/10.3390/molecules24071343

Petraglia, T., Latronico, T., Fanigliulo, A., Crescenzi, A., Liuzzi, G. M., & Rossano, R. (2023). Antioxidant Activity of Polysaccharides from the Edible Mushroom Pleurotus eryngii. *Molecules*, *28*(5), 2176. https://doi.org/10.3390/molecules28052176

Takaya, K., Asou, T., & Kishi, K. (2023). Cistanche deserticola Polysaccharide Reduces Inflammation and Aging Phenotypes in the Dermal Fibroblasts through the Activation of the NRF2/HO-1 Pathway. *International Journal of Molecular Sciences*, *24*(21), 15704. https://doi.org/10.3390/ijms242115704

Tian, X., Ao-Xun, Z., Wei-Ze, L., & Ping-Huai, L. (2023). Isolation, Purification, Chemical Composition and Antioxidant Activities of Polysaccharides from Dictyosphaerium sp.1A10. *Food Research and Development*, *44*(2), 57–65. https://doi.org/10.12161/j.issn.1005-6521.2023.02.009

Wei, J.-J., Li, X.-J., Liu, W., Chai, X.-J., Zhu, X.-Y., Sun, P.-H., Liu, F., Zhao, Y.-K., Huang, J.-L., Liu, Y.-F., & Zhao, S.-T. (2023). Eucommia Polysaccharides Ameliorate Aging-Associated Gut Dysbiosis: A Potential Mechanism for Life Extension in Drosophila. In *International Journal of Molecular Sciences* (Vol. *24*, Issue 6, p. 5881). https://doi.org/10.3390/ijms24065881

Yan, X., Miao, J., Zhang, B., Liu, H., Ma, H., Sun, Y., Liu, P., Zhang, X., Wang, R., Kan, J., Yang, F., & Wu, Q. (2023). Study on semi-bionic extraction of Astragalus polysaccharide and its anti-aging activity *in vivo*. In *Frontiers in Nutrition* (Vol. *10*, p. 1201919). https://doi.org/10.3389/fnut.2023.1201919

Yuan, H., Xu, Y., Luo, Y., Wang, N.-X., & Xiao, J.-H. (2021). Role of Nrf2 in cell senescence regulation. In *Molecular and Cellular Biochemistry* (Vol. *476*, Issue 1, pp. 247–259). https://doi.org/10.1007/s11010-020-03901-9

Zhao, D., Yan, M., Xu, H., Liang, H., Zhang, J., Li, M., & Wang, C. (2023). Antioxidant and Antiaging Activity of Fermented Coix Seed Polysaccharides on Caenorhabditis elegans. In *Nutrients* (Vol. *15*, Issue 11, p. 2474). https://doi.org/10.3390/nu15112474

Zhao, H., Xu,Q., & Zhou, H., (2017). Determination of uronic acid content in corn silk polysaccharide and study on its antioxidant effect. *Journal of Henan University of Technology*, *38*(04), 81–85. https://doi.org/10.16433/j.cnki.issn1673-2383.2017.04.015

Zou, X., BK, A., Abu-Izneid, T., Aziz, A., Devnath, P., Rauf, A., Mitra, S., Emran, T. B., Mujawah, A. A. H., Lorenzo, J. M., Mubarak, M. S., Wilairatana, P., & Suleria, H. A. R. (2021). Current advances of functional phytochemicals in Nicotiana plant and related potential value of tobacco processing waste: A review. *Biomedicine & Pharmacotherapy*, *143*, 112191. https://doi.org/10.1016/j.biopha.2021.112191